Manipulation of electronic property of epitaxial graphene on SiC substrate by Pb intercalation

Jinjin Wang,[1,2] Minsung Kim,[2] Liangyao Chen,[1] Kai-Ming Ho ,[2] Michael Tringides,[2]
Cai-Zhuang Wang,[2,*] and Songyou Wang[1,2,†]
[1]*Department of Optical Science and Engineering, Fudan University, Shanghai, 200433, China*
[2]*Ames Laboratory, US Department of Energy and Department of Physics, Iowa State University, Ames, Iowa 50011, USA*

(Received 25 September 2020; accepted 13 January 2021; published 2 February 2021;
corrected 3 February 2021)

Manipulating the electronic properties of graphene has been a subject of great interest since it can aid material design to extend the applications of graphene to many different areas. In this paper, we systematically investigate the effect of lead (Pb) intercalation on the structural and electronic properties of epitaxial graphene on the SiC(0001) substrate. We show that the band structure of Pb-intercalated few-layer graphene can be effectively tuned through changing intercalation conditions, such as coverage, location of Pb, and the initial number of graphene layers. Lead intercalation at the interface between the buffer layer (BL) and the SiC substrate decouples the BL from the substrate and transforms the BL into a *p*-doped graphene layer. We also show that Pb atoms tend to donate electrons to neighboring layers, leading to an *n*-doping graphene layer and a small gap in the Dirac cone under a sufficiently high Pb coverage. This paper provides useful guidance for manipulating the electronic properties of graphene layers on the SiC substrate.

DOI: 10.1103/PhysRevB.103.085403

I. INTRODUCTION

Graphene, a single atomic layer of carbon, has attracted considerable interest since its isolation in 2004 due to its outstanding physical properties, such as strong mechanical strength and superior electronic transport property [1–5]. Recently, it has been shown that the electronic and magnetic properties of graphene can be further manipulated by intercalation of other atomic or molecular species underneath the graphene [6–8].

Several experimental papers on Pb intercalation of graphene have been reported [9–15]. For example, Pb intercalation below graphene on Ir(111) was shown to induce magnetism in graphene because of the large spin-orbit coupling (SOC) [15]. The Pb-C interaction converts graphene to a two-dimensional (2D) electron gas in the presence of an effective magnetic field and produces unusually sharp Landau levels in the scanning-tunneling spectroscopy (STS) spectra [15]. A different paper on Pb intercalation on Pt(111) revealed the importance of the type of bonding site [13]. Angular resolved photo emission spectroscopy (ARPES) shows the splitting of the polarized graphene bands with a large band gap opening ∼200 meV [13]. In addition to metal substrates, graphene grown on 6H-SiC (0001) substrate has also been shown to be very promising for obtaining high-quality large-area graphene [16–20]. It is also a potential material for high-end electronics and promising for future high-frequency applications [21,22]. More possibilities to modify the band structure of graphene on SiC with heavy elements such as Pb intercalation exist but have not yet been well explored. One recent experimental paper shows that intercalation of Pb atoms under graphene on SiC leads to the *p*-doping character of the graphene layer, while it was known that pristine graphene on SiC exhibits *n*-doping [11]. Therefore, a systematic calculation of Pb intercalation under various graphene initial phases [i.e., buffer layer (BL), single layer and double layer graphene (SLG and DLG) on the SiC substrate] will provide useful insights for better understanding of the existing and future experimental results.

In this paper, we consider a system of one to three carbon layers (i.e., BL, SLG, and DLG) on a SiC(0001) substrate and systematically investigate the structural and electronic properties of the graphene layers at different Pb intercalation structures using first-principles calculations based on density functional theory (DFT). The changes induced by different intercalation conditions, including Pb coverage, location of Pb atoms whether on the SiC substrate or between the carbon layers, as well as the number of intercalation layers, are investigated and discussed. We show that Pb atoms intercalated under the BL can saturate the Si dangling bonds at the Si-terminated SiC(0001) surface, thus decoupling the BL from the SiC substrate and transforming the BL into a graphene layer. Moreover, the carrier type of the modified graphene layer can be tuned from *n* to *p* type or vice versa by changing Pb intercalation coverage. The effect of Pb intercalation on SLG and DLG on SiC has also been studied. With Pb atoms intercalated between the carbon layers, different effects on the band structure of graphene have been observed. As the number of intercalation layers increases, more graphene layers are decoupled from neighboring layers, resulting in the change of the number and position of the Dirac points in the system. According to our results, Pb atoms can help decouple graphene layers from neighboring layers, leading to the graphene band structure modifications in one system.

*wangcz@ameslab.gov
†songyouwang@fudan.edu.cn

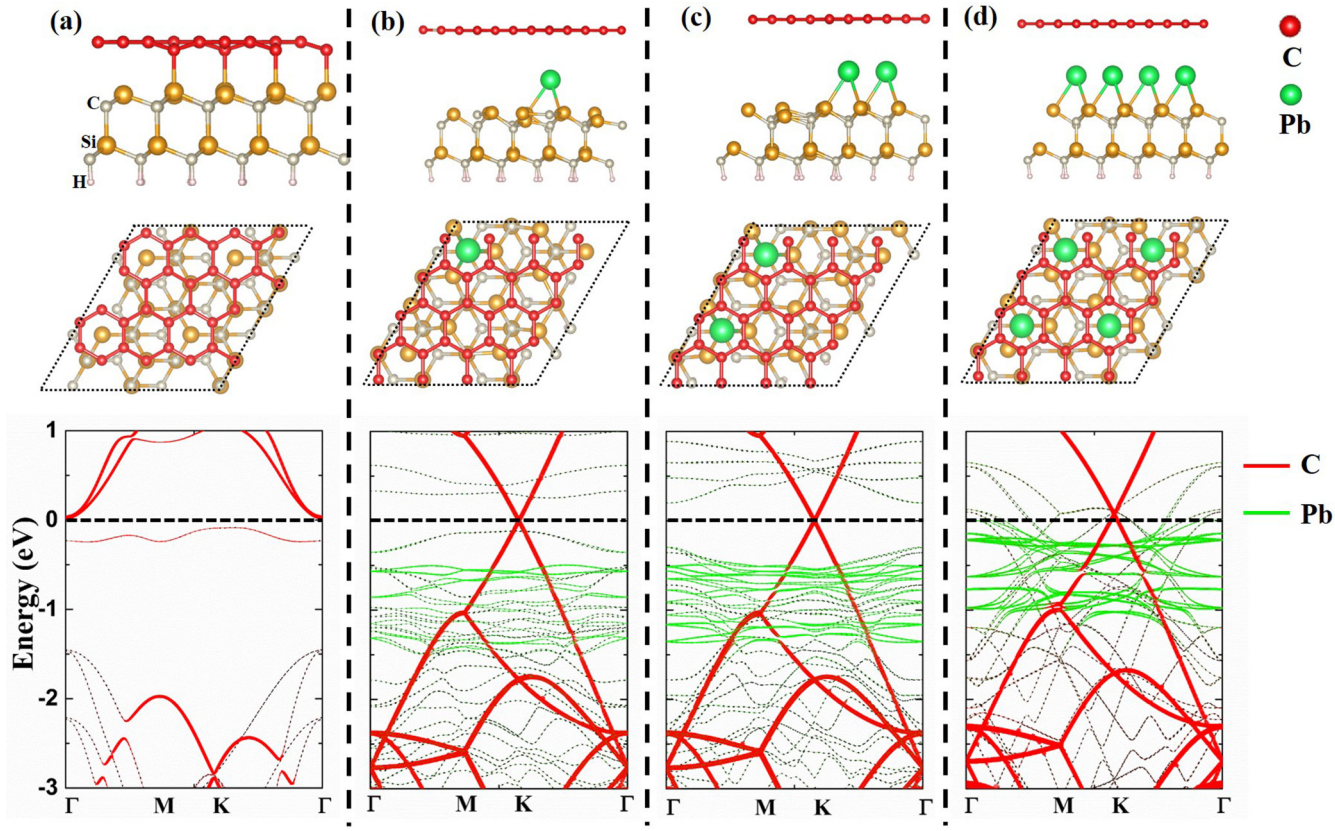

FIG. 1. The atomic configurations and corresponding projected electronic band structures contributed by carbon and lead p states in the Pb-intercalated buffer layer (BL) on SiC(0001) with Pb coverage of (a) 0 ML, (b) $\frac{1}{16}$ ML, (c) $\frac{1}{8}$ ML, and (d) $\frac{1}{4}$ ML at the BL-SiC interface. The Fermi level is set to 0 eV.

Thus, the electronic properties can be effectively modified by changing the intercalation condition.

II. COMPUTATIONAL METHODS

All calculations, including structural relaxation and electronic structure calculations, were carried out using first-principles DFT as implemented in the Vienna *ab initio* Simulation Package (VASP) [23]. Here, the projected augmented wave method was employed to describe the electron-ion interactions [24]. The generalized gradient approximation with the Perdew-Burke-Ernzerhof functional was adopted to evaluate the exchange-correlation potential [25]. The graphene on SiC system was modeled using two layers of SiC with $2 \times 2R30^\circ$ supercell as the substrate, topped with 4×4 graphene layers. The lattice mismatch was about 7.8% with the lattice constant of the SiC cell being compressed while the graphene layers kept their equilibrium lattice constant. To avoid the interactions between layers owing to the use of periodic boundary conditions, the thickness of the vacuum layer was set to be >15 Å. The bottom of the SiC slab was passivated by hydrogen atoms. The energy cutoff was 520 eV, and the van der Waals interaction was considered with the DFT-D3 method [26]. For structural relaxation, the total energy threshold was set as 10^{-6} eV/atom and the force was <0.01 eV/Å. In our calculations, a $6 \times 6 \times 1$ grid following the Monkhorst-Pack method [27] was used for k-point sampling.

The formation energy of the system is defined as

$$E_f = \frac{(NE_{\mathrm{Pb}} + E_0) - E_{\mathrm{total}}}{N}, \tag{1}$$

where N is the number of intercalated Pb atoms in the system, E_{Pb}, E_0, and E_{total} denote the energy of the bulk Pb (per atom), the initial system without Pb intercalation, and the Pb-intercalated system, respectively. Therefore, a positive value of formation energy E_f indicates the system is energetically favorable.

III. RESULTS AND DISCUSSION

A. Intercalation underneath the BL

For graphene grown on the SiC(0001) substrate, some atoms in the carbon layer next to the substrate form chemical bonds with the topmost silicon atoms of SiC. As a result, this layer exhibits different structure and electronic property from graphene and is usually named the BL. Figure 1(a) presents the geometric structure of BL on SiC and the corresponding projected band structure where the contribution of carbon p state in the BL is denoted by red lines. In Fig. 1, the dotted lines show the bands of the whole system, and the colored solid lines show the bands from corresponding atomic orbitals. In this case, the red and green lines in the band structures show the bands from the BL and Pb atoms, as shown in the figure, whose thicknesses represent the weight of the band eigenfunctions on different atomic orbitals. Intriguingly, the

TABLE I. The energies of Dirac points with respect to the Fermi level (E_{Dirac} in electronvolts), formation energy (E_f in electronvolts per atom), charge transfer of the carbon layer (Q_{C}) and intercalated Pb atoms (Q_{Pb}), and average interlayer distances (d_{I} in angstroms) with different Pb coverage at the buffer layer (BL)-SiC interface.

Pb coverage	0	$\frac{1}{16}$ ML	$\frac{1}{8}$ ML	$\frac{1}{4}$ ML	$\frac{9}{16}$ ML
E_{Dirac}		0.00	0.00	0.13	−0.42
E_f		0.05	0.81	0.92	0.46
Q_{C}	1.22e	0.04e	0.07e	0.00e	0.21e
Q_{Pb}		−0.24e	−0.21e	−0.19e	−0.76e
d_{I}	$d_{\text{C-Si}} = 2.35$	$d_{\text{C-Pb}} = 3.34$	$d_{\text{C-Pb}} = 3.34$	$d_{\text{C-Pb}} = 3.52$	$d_{\text{C-Pb}} = 3.57$
		$d_{\text{Pb-Si}} = 2.32$	$d_{\text{Pb-Si}} = 2.41$	$d_{\text{Pb-Si}} = 2.36$	$d_{\text{Pb-Si}} = 2.57$

typical graphene Dirac cone band dispersion is absent, leaving a large band gap of 1.5 eV and strong *n*-doping state caused by the strong covalent bonding between the BL and the Si atoms of the SiC substrate. The flat band just below the Fermi level is due to the unsaturated Si dangling bonds at the interface.

To explore the effects of Pb intercalation on the BL, intercalation with different Pb coverages beneath the BL was studied. The atomic configurations and associated projected band structures are shown in Figs. 1(b)–1(d) with Pb coverage as $\frac{1}{16}$, $\frac{1}{8}$, and $\frac{1}{4}$ ML (i.e., one Pb atom in 4 × 4, 4 × 2, and 2 × 2 graphene unit cells), respectively. In addition, Table I lists the energies of the Dirac point with respect to the Fermi level, the formation energies, the charge transfer of the BL and the intercalated Pb atoms, as well as the interlayer distances with different Pb coverages. From Fig. 1(b), we can see that the intercalated Pb atom bonds to the topmost Si atom, leading to the break of Si-C bonds at the interface, and thus decouples the BL from the SiC substrate. Under such a condition, the BL becomes an almost freestanding graphene layer, and the influence from the SiC substrate is substantially suppressed. Thus, a Dirac cone appears in its band structure, which is the main signature of graphene. When the Pb coverage increases, the Dirac cone shifts up and is 0.13 eV higher than the Fermi level for $\frac{1}{4}$ Pb coverage, indicating the conduction type changing from *n* to *p*. It was noted that hole doping can also be achieved by deposition of Pb on the top of the BL on SiC(0001) substrate, as reported in Ref. [28]. In addition, it is also found from Table I that the formation energy increases with Pb coverage, varying from 0 to $\frac{1}{4}$ ML, meaning that Pb intercalation becomes more energetically favorable with the increase of the Pb coverage owing to the increasing Pb-Si bonds.

There are two major effects of Pb intercalation at the BL-SiC interface: (i) on one hand, the covalent bonds between the substrate and the BL are broken, and the influence of SiC on the BL is suppressed through Pb intercalation. With the increase of intercalation coverage, the interaction between SiC and BL becomes weaker. Finally, the BL transforms into an almost freestanding graphene layer with Pb coverage at $\frac{1}{4}$ ML, which can be confirmed from the net atomic charge of the BL in Table I. The BL has negligible electron transfer with neighboring layers, implying that the BL is totally decoupled from the SiC substrate. (ii) On the other hand, electrons are transferred from the intercalated Pb layer to the graphene layer while they suppress the electron transfer from SiC to the graphene layer. This could be verified by the decrease of the Dirac point energy with the intercalation coverage increasing from $\frac{1}{4}$ to $\frac{9}{16}$ ML, i.e., nine atoms in a 4 × 4 graphene unit cell. The Dirac point energy drops below the Fermi level with the increasing intercalation coverage, demonstrating that Pb atoms donate electrons to BL and result in *n*-doped graphene within this Pb coverage range. Thus, both *p*- or *n*-conduction types can be obtained by changing the coverage of Pb intercalation, which demonstates that the electronic property of epitaxial graphene can be effectively tuned upon controlling Pb intercalation coverage.

B. Effects of Pb adsorption on intercalated graphene

Next, we studied the effect of an additional Pb atom absorbed on the top of the carbon layer after Pb was intercalated at the BL-SiC interface. The atomic configurations and corresponding projected band structures are presented in Fig. 2, with Table II providing detailed information including the Dirac point energies, the formation energies, the charge transfer of the BL and Pb atoms, and the interlayer distances.

As presented in Table II, the formation energy for an additional Pb atom adsorbed on the top of intercalated graphene is negative when the Pb intercalation coverage is $<\frac{1}{4}$ ML, implying that those configurations are not thermodynamically stable. Therefore, it can be inferred that it is energetically favorable for Pb atoms to intercalate underneath the carbon layer rather than adsorb on top when the Pb intercalation coverage is $<\frac{1}{4}$ ML, which is consistent with previous experimental results [11]. This is due to the weaker interaction between Pb and the graphene layer since Si atoms on the surface of SiC have more dangling bonds, whereas no dangling bond exists on the surface of a perfect graphene layer. As for the band structures, adoption of an Pb adatom introduces Pb flat bands just below the Fermi level, and these bands interact strongly with the graphene Dirac cone. All the structures with the Pb absorption exhibit *n*-type doping characteristics, even though the Pb intercalation reduces the charge transfer from SiC to the graphene layer. This is caused by the adsorption of the Pb atom on the top, which plays the role of electron donor to the graphene layer. Another notable feature of the band structures is that a small gap of ∼0.04 eV in the graphene Dirac cone appears with Pb adsorpbed in the $\frac{1}{8}$ ML Pb-intercalated structure, which is induced by the interaction between the graphene layer and the Pb adatom.

C. Intercalation of SLG

In addition to BL, cases with more graphene layers are investigated as well since SLG and DLG on SiC can be grown

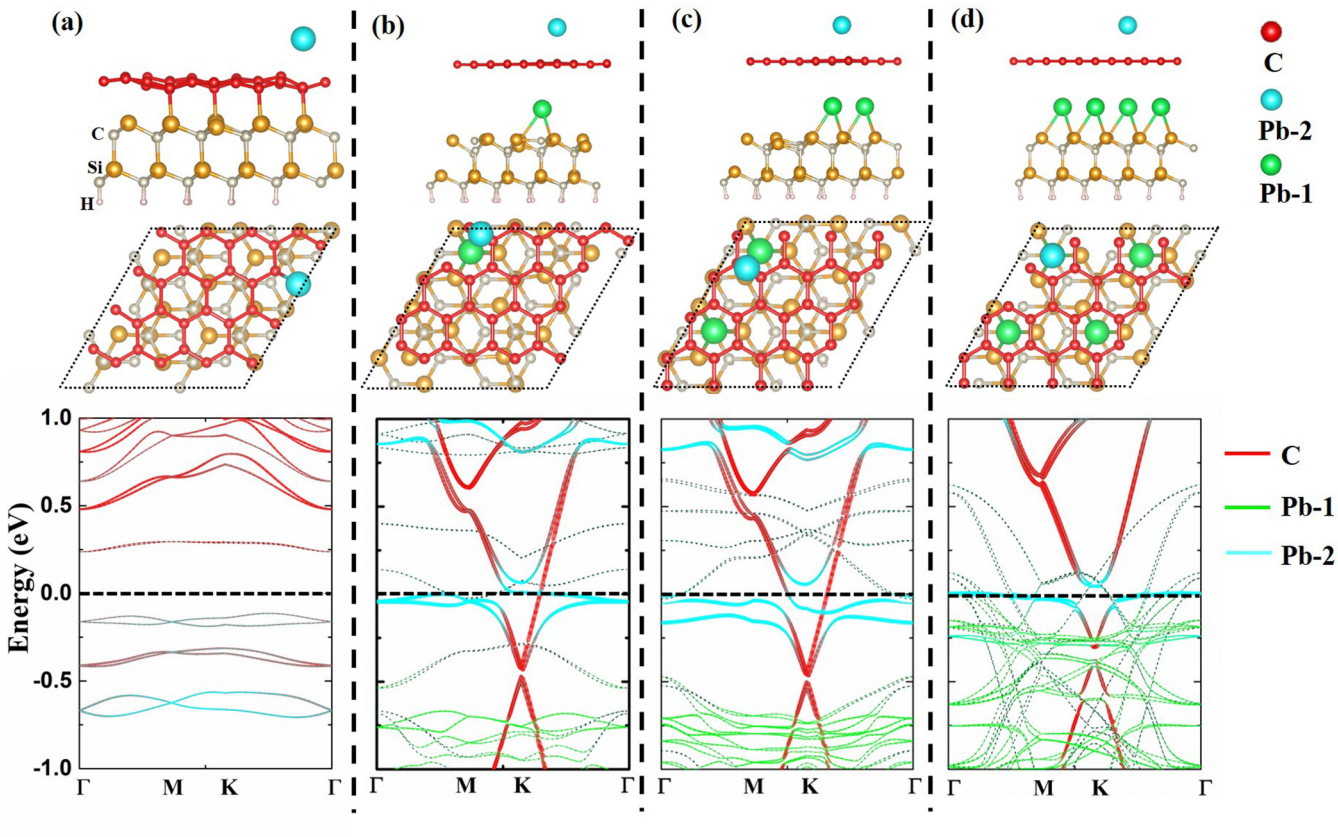

FIG. 2. The atomic configurations and corresponding projected electronic band structures contributed by carbon and lead p states in the Pb-intercalated buffer layer (BL) on SiC(0001) with Pb coverage of (a) 0 ML, (b) $\frac{1}{16}$ ML, (c) $\frac{1}{8}$ ML, and (d) $\frac{1}{4}$ ML at the BL-SiC interface, and with an extra Pb atom on top of graphene.

experimentally [11]. Figure 3 shows the atomic structures and electronic bands of Pb-intercalated single graphene from our calculations. We refer to the carbon layers from bottom to top in this system as BL and graphene layer, respectively, i.e., C-1 and C-2 shown in Fig. 3. Detailed information including the Dirac point energies, the formation energies, the charge state of the BL, the graphene layer and the Pb layers, as well as interlayer distances, are given in Table III.

Electronic energy band dispersion measured with ARPES along the Γ-K-M high symmetry direction in the graphene Brillouin zone for an epitaxial SLG on SiC(0001) surface has been reported in Ref. [11]. Before Pb intercalation, a Dirac cone with a small gap and the Dirac point about 0.42 eV below the Fermi level has been shown by ARPES spectrum. Our result is consistent with the experimental result, as shown in Fig. 3(a). There is a Dirac cone below the Fermi level about 0.58 eV with a small gap of 0.12 eV, while the BL is still bonded to the SiC substrate in the absence of Pb intercalation. With Pb intercalated at the BL-SiC interface, two linear Dirac cones with strong hybridization appear in the vicinity of the Fermi level in Fig. 3(b), as expected in AB-stacked bilayer graphene, owing to the decoupling of the BL from

TABLE II. The energies of Dirac points with respect to the Fermi level (E_{Dirac} in electronvolts) and with the gap value shown in the bracket, formation energy (E_f in electronvolts per atom), charge transfer of the carbon layer (Q_{C}) and Pb atoms in different layers ($Q_{\text{Pb-1}}$ and $Q_{\text{Pb-2}}$), as well as average interlayer distances (d_{I} in angstroms) at different Pb intercalation coverages at the buffer layer (BL)-SiC interface (the Pb coverage on the top of the BL is fixed at $\frac{1}{16}$ ML since only one Pb adatom is added to the supercell).

Pb coverage	0	$\frac{1}{16}$ ML	$\frac{1}{8}$ ML	$\frac{1}{4}$ ML
E_{Dirac}		−0.46 (0.05)	−0.48 (0.04)	−0.36 (0.11)
E_f	−1.89	−1.28	−0.33	0.38
Q_{C}	6.00e	0.23e	0.35e	0.20e
$Q_{\text{Pb-1}}$		−0.21e	−0.41e	−0.73e
$Q_{\text{Pb-2}}$	−0.46e	−0.24e	−0.36e	−0.29e
d_{I}	$d_{\text{Pb-C}} = 2.44$	$d_{\text{Pb2-C}} = 2.73$	$d_{\text{Pb2-C}} = 2.72$	$d_{\text{Pb2-C}} = 2.70$
	$d_{\text{C-Si}} = 2.29$	$d_{\text{C-Pb1}} = 3.33$	$d_{\text{C-Pb1}} = 3.40$	$d_{\text{C-Pb1}} = 3.45$
		$d_{\text{Pb1-Si}} = 2.37$	$d_{\text{Pb1-Si}} = 2.46$	$d_{\text{Pb1-Si}} = 2.34$

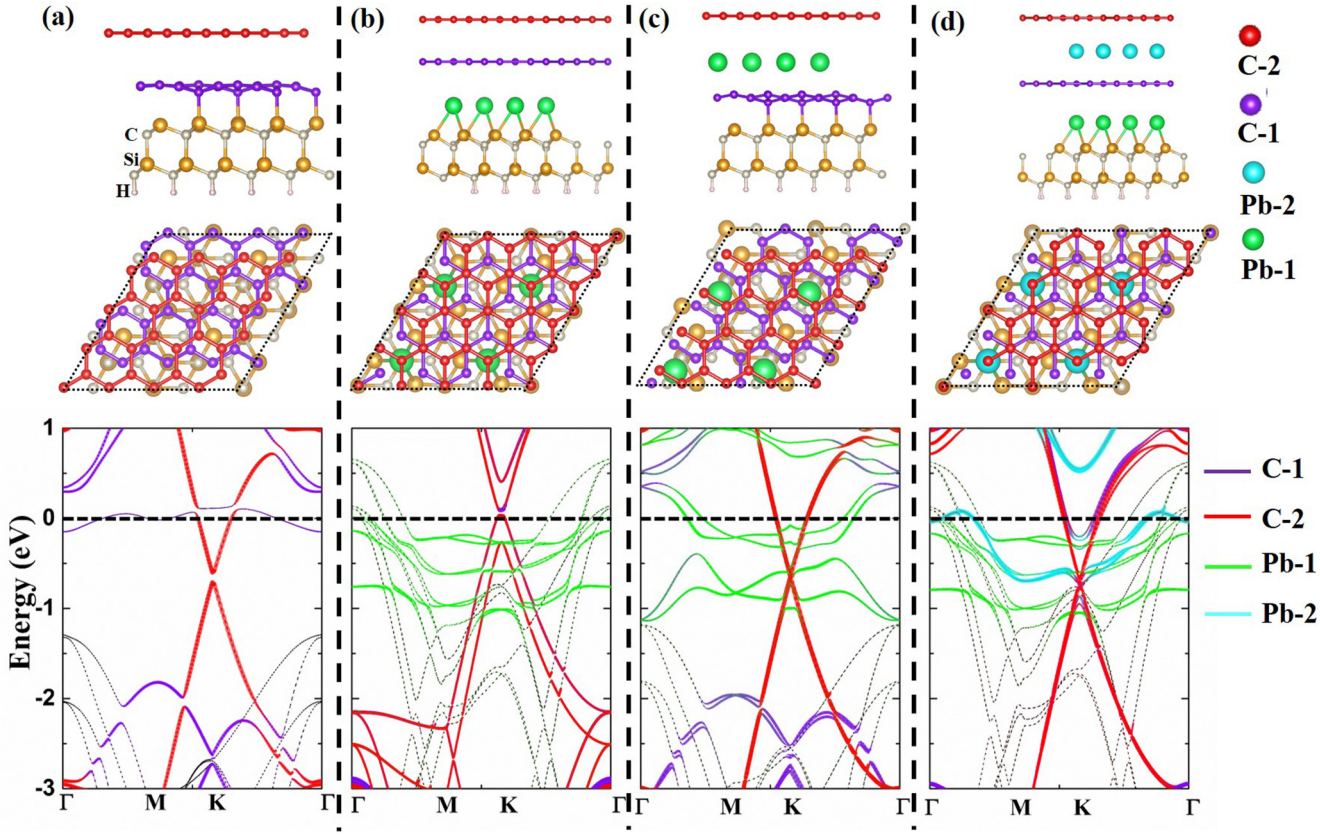

FIG. 3. The atomic configurations and corresponding projected electronic band structures contributed by carbon and lead p states in Pb-intercalated single layer graphene (SLG) on SiC(0001) with intercalation coverage of (a) 0 Pb, (b) $\frac{1}{4}$ ML of Pb under the buffer layer (BL), (c) $\frac{1}{4}$ ML of Pb under the graphene layer, and (d) $\frac{1}{4}$ ML of Pb in both layers.

the substrate which transforms the BL into a graphene layer. The ARPES spectrum shows two additional Dirac cones with one Dirac point slightly below and another slightly above the Fermi level, which is consistent with our calculations. Therefore, our calculations suggest that the experimental sample in Ref. [11] consists of mixed nonintercalated SLG domains and Pb-intercalated DLG domains with Pb intercalated between the BL-SiC interface. It was noted that the Moiré pattern has also been observed in Ref. [11] and has been attributed to the interface mismatch between the intercalated Pb layer and the BL. However, calculations for structures with a Moiré pattern will require a much larger unit cell which is a challenge for first-principles methods and out of scope of the present calculations.

If the Pb intercalation is not underneath the BL but rather under the graphene layer, as shown in Fig. 3(c), the electronic structures are dramatically different. Corresponding electronic structure exhibits only a single Dirac cone with the Dirac point about 0.64 eV below the Fermi level. This is because the Pb intercalation decouples the interaction between

TABLE III. The energies of Dirac points with respect to the Fermi level (E_{Dirac} in electronvolts) and with the gap value shown in the bracket, formation energy (E_f in electronvolts per atom), charge transfer of the buffer layer ($Q_{\text{C-1}}$), graphene layer ($Q_{\text{C-2}}$), and Pb atoms in different interaction layers (Q_{Pb}), as well as average interlayer distances (d_{I} in angstroms) at different Pb positions. Each column corresponds to the location of the intercalared Pb.

Pb position	0	Lower	Upper	Both
E_{Dirac}	−0.58 (0.12)	0.06 (0.06)	−0.64	−0.71
E_f		3.03	0.67	0.46
$Q_{\text{C-1}}$	1.31e	0.01e	1.62e	0.10e
$Q_{\text{C-2}}$	0.01e	0.00e	0.09e	0.14e
Q_{Pb}		−0.22e	−0.48e	−0.15e −0.29e
d_{I}	$d_{\text{C1-C0}} = 3.43$ $d_{\text{C0-Si}} = 2.31$	$d_{\text{C1-C0}} = 3.36$ $d_{\text{C0-Pb}} = 3.51$ $d_{\text{Pb-Si}} = 2.36$	$d_{\text{C1-Pb}} = 3.36$ $d_{\text{Pb-C0}} = 2.61$ $d_{\text{C0-Si}} = 2.29$	$d_{\text{C1-Pb2}} = 3.04$ $d_{\text{Pb2-C0}} = 2.96$ $d_{\text{C0-Pb1}} = 3.56$ $d_{\text{Pb1-Si}} = 2.34$

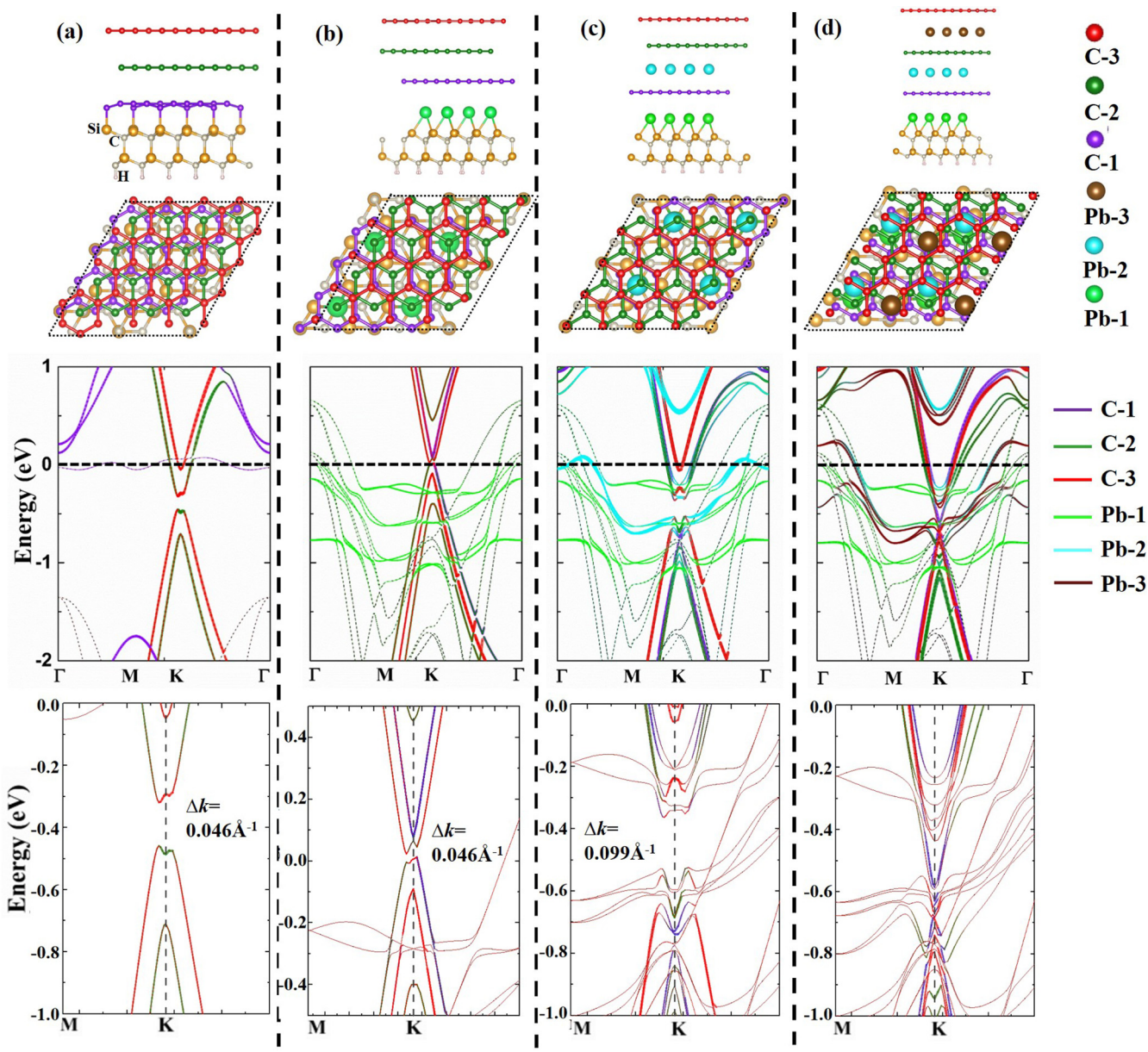

FIG. 4. The atomic structures and corresponding projected electronic band structures contributed by carbon and lead p states in Pb-intercalated double layer graphene (DLG) on SiC(0001) with intercalation coverage of (a) 0 Pb, (b) $\frac{1}{4}$ ML of Pb in the lower intercalation layer, (c) $\frac{1}{4}$ ML of Pb in both the buffer layer (BL) and the middle carbon layer (C-2), and (d) $\frac{1}{4}$ ML of Pb under all three carbon layers. The band structures shown in the bottom panels are the zoom-in version of the bands to shown the horizontal splitting of the Dirac cones more clearly.

the graphene and the BL and removes the small gap in the Dirac cone. Therefore, Pb-intercalation position is vital for manipulating the electronic properties of graphene layers.

When both the BL and graphene layers are intercalated with Pb, as shown in Fig. 3(d), the BL also turns into another monolayer graphene which has almost the same net atomic charge as the graphene layer. Therefore, two Dirac cones from the two individual graphene layers show overlap. The energy of the Dirac cone shifts downward to −0.71 eV as compared with that of the single layer intercalated under the graphene layer (which is −0.64 eV). This is caused by the fact that Pb atoms donate electrons to neighboring graphene layers, which can be further confirmed by the net atomic charge in Table III. Therefore, changing the number of intercalation layers can be an effective way to modulate the Dirac cones and conduction type of the graphene layers.

D. Intercalation of DLG

As for the case with DLG (which involves three layers, i.e., the BL, the SLG, and the DLG from bottom to top, i.e., C-1, C-2, and C-3 in Fig. 4) on the SiC substrate, the calculated results are shown in Fig. 4 and Table IV. Without Pb intercalation, the system can be seen as two components: a BL with the SiC substrate and an AB-stacked bilayer graphene above the BL. The overall feature of the electronic band structure

TABLE IV. The energies of Dirac points with respect to the Fermi level (E_{Dirac} in electronvolts) and with the gap value in the bracket, formation energy (E_f in electronvolts per atom), charge transfer of the buffer layer (Q_{C}), graphene layer ($Q_{\text{C-1}}$ and $Q_{\text{C-2}}$), and Pb atoms (Q_{Pb}), as well as average interlayer distances (d_{I} in angstroms) with different Pb intercalation structures. The distances are given from the position of the intercalated Pb atoms at a given location to the layers above and below the atom. The different configurations and Pb amounts are seen in Figs. 4(a)–4(d).

Pb intercalation layers	0	1	2	3
E_{Dirac}	−0.39 (0.20)	0.01 (0.01)	−0.46 (0.45)	−0.67
E_f		0.37	−0.87	−1.25
Q_{C}	1.19e	0.01e	0.11e	0.08e
$Q_{\text{C-1}}$	0.03e	0.00e	0.12e	0.28e
$Q_{\text{C-2}}$	0.02e	0.00e	0.03e	0.11e
Q_{Pb}		0.22e	−0.16e	−0.16e
			−0.31e	−0.28e
				−0.24e
d_{I}	$d_{\text{C2-C1}} = 3.38$	$d_{\text{C2-C1}} = 3.42$	$d_{\text{C2-C1}} = 3.35$	$d_{\text{C2-Pb3}} = 3.17$
	$d_{\text{C1-C0}} = 3.41$	$d_{\text{C1-C0}} = 3.41$	$d_{\text{C1-Pb2}} = 3.02$	$d_{\text{Pb3-C1}} = 3.04$
	$d_{\text{C0-Si}} = 2.34$	$d_{\text{C0-Pb}} = 3.53$	$d_{\text{Pb2-C0}} = 2.94$	$d_{\text{C1-Pb2}} = 2.93$
		$d_{\text{Pb-Si}} = 2.36$	$d_{\text{C0-Pb1}} = 3.37$	$d_{\text{Pb2-C0}} = 3.10$
			$d_{\text{Pb1-Si}} = 2.33$	$d_{\text{C0-Pb1}} = 3.57$
				$d_{\text{Pb1-Si}} = 2.34$

from the two graphene layers follows that of bilayer graphene, similar to that in Fig. 3(b) but with a subtle difference. The difference is that the extreme points of the parabola of the Dirac cones exhibit a small horizontal splitting ($\Delta k = 0.046\,\text{Å}^{-1}$) in addition to the vertical splitting of about 0.13 eV, as seen in the zoom-in band structure shown in the bottom panel in Fig. 4(a). In Fig. 4(b), Pb atoms intercalated under the BL decouple the BL from the SiC substrate, resulting in a trilayer graphene system. Note that the corresponding band structure shows the feature of ABA-stacked trilayer graphene. A small horizontal splitting of $\Delta k = 0.046\,\text{Å}^{-1}$ is also observed near the Dirac cones, but the vertical splitting is much smaller than that in Fig. 4(a), as shown more clearly in the bottom panel of Fig. 4(b). When both the BL and the middle graphene layer are intercalated, the middle graphene layer is separated from the BL, and the top two carbon layers form an AB-stacked bilayer graphene. Here, we can see that the electronic bands of the BL share similar features with those of the middle graphene layer, which is caused by their nearly identical net atomic charge. Interestingly, both horizontal and vertical splittings of the Daric point are significantly large in this intercalation configuration, as clearly shown in the bottom panel of Fig. 4(c). The horizontal splitting is about $\Delta k = 0.10\,\text{Å}^{-}1$, and the verticle splitting is 0.16 eV. With Pb intercalated in all three layers, the carbon layers turn into three separate graphene layers. Here, the BL exhibits similar band structure as the top (C-3) graphene, while the band structure from the middle layer (C-2) is different. These results also demonstrate that the properties of Dirac cones can be easily modified through controlling the number of Pb-intercalation layers.

E. Discussion

Intercalated graphene with various elements such as H [29], O [30], F [31], Si [32], Li [33], transition-metals (TMs) [34–38], and rare earth metals [39–41] have been reported in the literature. Impacts on the structural and electronic properties of graphene are strongly dependent on the strength of the interactions between graphene and the intercalated atoms, as well as the intercalation geometries. It was found that epitaxial BL turns into a quasifreestanding graphene layer with an atom intercalated atop the SiC substrate for most of the intercalation configurations. However, effects of the intercalation on the electronic structure of the graphene can be different with different intercalation location and geometry. For example, *p*-doped graphene and a shift of the Dirac point above the Fermi level have been observed for O and F intercalation of graphene on SiC(0001) [30,31]. On the other hand, electron doping of graphene and lowering of the Dirac point with respect to the Fermi level have been reported for Li intercalation [33]. Because the interaction between graphene and TMs are strong, the modifications in the electronic and magnetic properties of graphene upon TM intercalation are more significant. It has been reported that the experimentally accessible Mn-intercalated epitaxial graphene on SiC(0001) transforms into a Dirac half metal when the coverage is more than $\frac{1}{3}$ ML [37]. Moreover, presence of multiple spin-polarized *p* bands in the Fe-intercalated bilayer graphene has also been reported [38].

It was reported that the interaction between Pb and graphene is almost the weakest among all metal atoms [11]. Our present calculations show that the effects of Pb intercalation on the structural and electronic properties of graphene are different from TM intercalations. According to our calculations, Pb not only decouples the BL from the SiC substrate but also suppresses the electron transfer from the substrate to the BL. Moreover, an energy gap can be opened for the Dirac cone of monolayer graphene under strong charge transfer. When the number of intercalated graphene layers increases, more bands and Dirac cones are present. The interactions between the Dirac cones from different graphene layers not only split the Dirac point vertically but also introduce a small horizontal shift of the Dirac point. We believe that our systematic calculations of Pb intercalations in various graphene configurations

(BL, SLG, and DLG) can help advance the understanding of electronic properties of graphene layers under Pb intercalation and provide theoretical support for experimental engineering of the band structure.

Due to the limitation of the number of atoms that can be handled in first-principles calculations, well-ordered structures for Pb intercalation are used in our calculations. These intercalated structures would be different from the real structures in the experiment, where some small amount of disorder remains in the experimental system. In principle, the outcome of intercalation in the experiment depends on the initial deposited amount, the annealing temperature used to transfer the deposited metal from the top to below the graphene, and the annealing time. One expects that, for a sufficiently large amount of deposited metal and high enough temperature, more uniform phases will form. For incomplete annealing, mixed phases would coexist. From our studies, we found the interaction between Pb and graphene is very weak; the major effects of Pb intercalation are to decouple the BL from the SiC substrate and to change electron transfer between the Pb and graphene layer to modify the locations of the Dirac cones with respect to the Fermi level. In this regard, the effects of possible disorder in the intercalation layer would not be significant. Since our calculations provide the band structures for different Pb-intercalated structures, experimental ARPES spectra can be compared with the calculated band structures to identify the atomic structures of the corresponding intercalations. For sufficiently high temperatures, uniform intercalated phases are expected; if not, then one would observe broader ARPES energy dispersions and lower relative intensities due to the inhomogeneity, but the basic features will be recognizable. For example, our calculated results shown in Figs. 3(a) and 3(b) can be used to explain the experimental ARPES spectrum from the sample of Pb-intercalated graphene on SiC(0001) reported in Ref. [11] and help to identify the structure in the experimental sample as mixed nonintercalated SLG and Pb-intercalated DLG domains with Pb intercalation between the BL-SiC substrate.

IV. CONCLUSIONS

In summary, we have systematically investigated the structural and electronic properties of Pb-intercalated epitaxial graphene on the SiC(0001) substrate through first-principles calculations. Our results demonstrate that Pb intercalation can be an effective way to manipulate the electronic properties, especially the Dirac cone positions and separations of graphene layers. It is confirmed that Pb atoms at the BL-SiC interface form bonds with Si atoms on the SiC surface and therefore decouple the BL from the substrate. In addition, Pb atoms are determined to be more energetically favorable to intercalate beneath the BL rather than under other graphene layers. The electron transfer from the substrate to the BL is suppressed upon Pb intercalation, leading to the change of the BL carrier type from *n* to *p*. In addition, the Pb atom adsorbed on the top of graphene also plays the role of electron donor and turns graphene into *n*-doping again depending on the coverage. Moreover, the Dirac cone bands of monolayer graphene can open a gap under strong charge transfer. With the number of Pb intercalation layers increasing, more graphene layers are separated, leading to a large number of bands and Dirac cones. Our findings can deepen the understanding of electronic properties of graphene layers under Pb intercalation and pave the way for their experimental realization.

ACKNOWLEDGMENTS

Work at Ames Laboratory was supported by the U.S. Department of Energy (US), Office of Science, Basic Energy Sciences, Materials Science and Engineering Division, including a grant of computer time at the National Energy Research Scientific Computing Centre (US) in Berkeley, CA. Ames Laboratory is operated for the U.S. DOE by Iowa State University under Contract No. DE-AC02-07CH11358. J. J. Wang and S. Y. Wang were also partially supported by the National Natural Science Foundation of China (CN) (Grant No. 11374055).

[1] A. K. Geim and K. S. Novoselov, The rise of graphene, Nat. Mater. **6**, 183 (2007).

[2] A. H. Castro Neto, F. Guinea, N. M. R. Peres, K. S. Novoselov, and A. K. Geim, The electronic properties of graphene, Rev. Mod. Phys. **81**, 109 (2009).

[3] A. K. Geim, Graphene: status and prospects, Science **324**, 1530 (2009).

[4] K. S. Novoselov, A. K. Geim, S. V. Morozov, D. Jiang, M. I. Katsnelson, I. V. Grigorieva, S. V. Dubonos, and A. A. Firsov, Two-dimensional gas of massless Dirac fermions in graphene, Nature **438**, 197 (2005).

[5] A. C. Ferrari, J. C. Meyer, V. Scardaci, C. Casiraghi, M. Lazzeri, F. Mauri, S. Piscanec, D. Jiang, K. S. Novoselov, S. Roth, and A. K. Geim, Raman Spectrum of Graphene and Graphene Layers, Phys. Rev. Lett. **97**, 187401 (2006).

[6] N. Rougemaille, A. T. N'Diaye, J. Coraux, C. Vo-Van, O. Fruchart, and A. K. Schmid, Perpendicular magnetic anisotropy of cobalt films intercalated under graphene, Appl. Phys. Lett. **101**, 142403 (2012).

[7] U. Starke, S. Forti, K. V. Emtsev, and C. Coletti, Engineering the electronic structure of epitaxial graphene by transfer doping and atomic intercalation, MRS Bull. **37**, 1177 (2012).

[8] C. Riedl, C. Coletti, and U. Starke, Structural and electronic properties of epitaxial graphene on SiC(0 0 0 1): A review of growth, characterization, transfer doping and hydrogen intercalation, J. Phys. D Appl. Phys. **43**, 374009 (2010).

[9] L. Jin, Q. Fu, R. Mu, D. Tan, and X. Bao, Pb intercalation underneath a graphene layer on Ru(0001) and its effect on graphene oxidation, Phys. Chem. Chem. Phys. **13**, 16655 (2011).

[10] X. Fei, L. Zhang, W. Xiao, H. Chen, Y. Que, L. Liu, K. Yang, S. Du, and H.-J. Gao, Structural and electronic properties of Pb-intercalated graphene on Ru(0001), J. Phys. Chem. C **119**, 9839 (2015).

[11] A. Yurtsever, J. Onoda, T. Iimori, K. Niki, T. Miyamachi, M. Abe, S. Mizuno, S. Tanaka, F. Komori, and Y. Sugimoto, Effects of Pb intercalation on the structural and electronic properties of epitaxial graphene on SiC, Small **12**, 3956 (2016).

[12] D. A. Estyunin, I. I. Klimovskikh, V. Y. Voroshnin, D. M. Sostina, L. Petaccia, G. Di Santo, and A. M. Shikin, Formation of a quasi-free-standing graphene with a band gap at the dirac point by Pb atoms intercalation under graphene on Re(0001), J. Exp. Theor. Phys. **125**, 762 (2017).

[13] I. I. Klimovskikh, M. M. Otrokov, V. Y. Voroshnin, D. Sostina, L. Petaccia, G. Di Santo, S. Thakur, E. V. Chulkov, and A. M. Shikin, Spin-orbit coupling induced gap in graphene on Pt(111) with intercalated pb monolayer, ACS Nano **11**, 368 (2017).

[14] I. Shtepliuk, M. Vagin, I. G. Ivanov, T. Iakimov, G. R. Yazdi, and R. Yakimova, Lead (Pb) interfacing with epitaxial graphene, Phys. Chem. Chem. Phys. **20**, 17105 (2018).

[15] F. Calleja, H. Ochoa, M. Garnica, S. Barja, J. J. Navarro, A. Black, M. M. Otrokov, E. V. Chulkov, A. Arnau, A. L. Vázquez de Parga, F. Guinea, and R. Miranda, Spatial variation of a giant spin-orbit effect induces electron confinement in graphene on Pb islands, Nat. Phys. **11**, 43 (2014).

[16] M. Hupalo, E. H. Conrad, and M. C. Tringides, Growth mechanism for epitaxial graphene on vicinal 6H-SiC(0001) surfaces: A scanning tunneling microscopy study, Phys. Rev. B **80**, 041401(R) (2009).

[17] N. Mishra, J. Boeckl, N. Motta, and F. Iacopi, Graphene growth on silicon carbide: A review, Phys. Status Solidi A **213**, 2277 (2016).

[18] T. W. Hu, X. T. Liu, F. Ma, D. Y. Ma, K. W. Xu, and P. K. Chu, High-quality, single-layered epitaxial graphene fabricated on 6H-SiC (0001) by flash annealing in Pb atmosphere and mechanism, Nanotechnology **26**, 105708 (2015).

[19] W. Choi, I. Lahiri, R. Seelaboyina, and Y. S. Kang, Synthesis of graphene and its applications: A review, Crit. Rev. Solid State **35**, 52 (2010).

[20] W. A. de Heer, C. Berger, M. Ruan, M. Sprinkle, X. Li, Y. Hu, B. Zhang, J. Hankinson, and E. Conrad, Large area and structured epitaxial graphene produced by confinement controlled sublimation of silicon carbide, P. Natl. Acad. Sci. **108**, 16900 (2011).

[21] M. Ruan, Y. Hu, Z. Guo, R. Dong, J. Palmer, J. Hankinson, C. Berger, and W. A. de Heer, Epitaxial graphene on silicon carbide: introduction to structured graphene, MRS Bull. **37**, 1138 (2012).

[22] Y.-M. Lin, C. Dimitrakopoulos, K. A. Jenkins, H.-Y. Chiu, and A. Grill, P. Avouris, 100-GHz transistors from wafer-scale epitaxial graphene, Science **327**, 662 (2010).

[23] G. Kresse and J. Furthmuller, Efficient iterative schemes for ab initio total-energy calculations using a plane-wave basis set, Phys. Rev. B **54**, 11169 (1996).

[24] P. E. Blöchl, Projector augmented-wave method, Phys. Rev. B **50**, 17953 (1994).

[25] J. P. Perdew, K. Burke, and M. Ernzerhof, Generalized Gradient Approximation Made Simple, Phys. Rev. Lett. **77**, 3865 (1996).

[26] S. Grimme, J. Antony, S. Ehrlich, and H. Krieg, A consistent and accurate *ab initio* parametrization of density functional dispersion correction (DFT-D) for the 94 elements H-Pu, J. Chem. Phys. **132**, 154104 (2010).

[27] D. J. Chadi, Special points for Brillouin-zone integrations, Phys. Rev. B **16**, 1746 (1977).

[28] Y. Tsujikawa, M. Sakamoto, Y. Yokoi, M. Imamura, K. Takahashi, R. Hobara, T. Uchihashi, and A. Takayama, Controlling of the Dirac band states of Pb-deposited graphene by using work function difference, AIP Adv. **10**, 085314 (2020).

[29] C. Riedl, C. Coletti, T. Iwasaki, A. A. Zakharov, and U. Starke, Quasi-Free-Standing Epitaxial Graphene on SiC Obtained by Hydrogen Intercalation, Phys. Rev. Lett. **103**, 246804 (2009).

[30] M. H. Oliveira, T. Schumann, F. Fromm, R. Koch, M. Ostler, M. Ramsteiner, T. Seyller, J. M. J. Lopes, and H. Riechert, Formation of high-quality quasi-free-standing bilayer graphene on SiC(0001) by oxygen intercalation upon annealing in air, Carbon **52**, 83 (2013).

[31] A. L. Walter, K.-J. Jeon, A. Bostwick, F. Speck, M. Ostler, T. Seyller, L. Moreschini, Y. S. Kim, Y. J. Chang, K. Horn, and E. Rotenberg, Highly *p*-doped epitaxial graphene obtained by fluorine intercalation, Appl. Phys. Lett. **98**, 184102 (2011).

[32] M. G. Silly, M. D'Angelo, A. Besson, Y. J. Dappe, S. Kubsky, G. Li, F. Nicolas, D. Pierucci, and M. Thomasset, Electronic and structural properties of graphene-based metal-semiconducting heterostructures engineered by silicon intercalation, Carbon **76**, 27 (2014).

[33] C. Virojanadara, S. Watcharinyanon, A. A. Zakharov, and L. I. Johansson, Epitaxial graphene on 6H-SiC and Li intercalation, Phys. Rev. B **82**, 205402 (2010).

[34] Y. Li, P. Chen, G. Zhou, J. Li, J. Wu, B. L. Gu, S. B. Zhang, and W. Duan, Dirac Fermions in Strongly Bound Graphene Systems, Phys. Rev. Lett. **109**, 206802 (2012).

[35] T. Gao, Y. Gao, C. Chang, Y. Chen, M. Liu, S. Xie, K. He, X. Ma, Y. Zhang, and Z. Liu, Atomic-scale morphology and electronic structure of manganese atomic layers underneath epitaxial graphene on SiC(0001), ACS Nano **6**, 6562 (2012).

[36] M. Upadhyay Kahaly, T. P. Kaloni, and U. Schwingenschlögl, Pseudo Dirac dispersion in Mn-intercalated graphene on SiC, Chem. Phys. Lett. **578**, 81 (2013).

[37] Y. Li, D. West, H. Huang, J. Li, S. B. Zhang, and W. Duan, Theory of the Dirac half metal and quantum anomalous Hall effect in Mn-intercalated epitaxial graphene, Phy. Rev. B **92**, 201403(R) (2015).

[38] S. J. Sung, J. W. Yang, P. R. Lee, J. G. Kim, M. T. Ryu, H. M. Park, G. Lee, C. C. Hwang, K. S. Kim, J. S. Kim, and J. W. Chung, Spin-induced band modifications of graphene through intercalation of magnetic iron atoms, Nanoscale **6**, 3824 (2014).

[39] N. A. Anderson, M. Hupalo, D. Keavney, M. Tringides, and D. Vaknin, Intercalated rare-earth metals under graphene on SiC, J. Magn. Magn. Mater. **474**, 666 (2019).

[40] M. Kim, M. C. Tringides, M. T. Hershberger, S. Chen, M. Hupalo, P. A. Thiel, C.-Z. Wang, and K.-M. Ho, Manipulation of Dirac cones in intercalated epitaxial graphene, Carbon **123**, 93 (2017).

[41] S. Watcharinyanon, L. I. Johansson, C. Xia, J. Ingo Flege, A. Meyer, J. Falta, and C. Virojanadara, Ytterbium intercalation of epitaxial graphene grown on Si-face SiC, Graphene **2**, 66 (2013).

Correction: The name of the second author was spelled incorrectly and has been fixed.